

(1970).

³A. M. Ermolaev and G. B. Sochilin, *Dokl. Akad. Nauk* **155**, 1050 (1964) [*Sov. Phys. Dokl.* **9**, 292 (1964)]; W. G. Cooper and D. J. Kouri, *J. Chem. Phys.* **57**, 2487 (1972); J. Macek, *J. Phys. B: Proc. Phys. Soc., London* **1**, 831 (1968).

⁴D. L. Knirk, *J. Chem. Phys.* **60**, 66 (1974).

⁵D. L. Knirk, *J. Chem. Phys.* **60**, 760 (1974).

⁶D. L. Knirk, "Solution by Recursion of the N -Body Electrostatic Schrödinger Equation" (to be published).

⁷M. Kotani, A. Amemiya, E. Ishiguro, and T. Kimura, *Tables of Molecular Integrals* (Maruzen Co., Ltd., Tokyo, 1963), Chap. 1.

⁸M. Hamermesh, *Group Theory* (Addison-Wesley, Reading, Mass., 1962), p. 99.

⁹Specifically, for 2S lithium, the wave function must behave as r^2 at the origin, but the analysis of Demkov and Ermolaev leads to a r^0 behavior. See Ref. 6.

¹⁰See Macek, Ref. 3. This method is currently being applied to helium by C. D. Lin and U. Fano at the University of Chicago.

¹¹C. M. Rosenthal and E. B. Wilson, *Phys. Rev. Lett.* **19**, 143 (1967); D. Macolm, *Phys. Rev. A* **7**, 1272 (1973).

¹²A. K. Bhatia and R. N. Madan, *Phys. Rev. A* **7**, 523 (1973); see also Cooper and Kouri, Ref. 3.

Conversion of Electromagnetic Waves to Electrostatic Waves in Inhomogeneous Plasmas*

R. L. Stenzel, A. Y. Wong, and H. C. Kim†

TRW Systems, Redondo Beach, California 90278, and Department of Physics, University of California at Los Angeles, Los Angeles, California 90024

(Received 23 October 1973)

Propagation of electromagnetic waves in a large plasma reveals that refraction effects are much more significant than the amplitude swelling commonly predicted from the reduction in group velocity. Near electromagnetic wave cutoff, direct conversion into short-wavelength electron plasma waves is observed. Strong resonant enhancement of the electric field parallel to the density gradient is measured.

Recently considerable attention has been focused¹ on the propagation of electromagnetic (EM) waves in nonuniform plasmas near the cutoff region where the incident frequency ω is close to the local electron plasma frequency ω_p . Near cutoff the conversion² to large-amplitude electrostatic (ES) electron plasma waves of short wavelengths can take place, which can effectively transfer energy to plasma particles. The basic understanding of these processes is crucial to the study of laser-plasma interactions as well as the large-scale modification of the ionosphere by EM waves. In this paper, we present experimental data on such processes obtained in a plasma whose dimensions are much larger than the free-space EM wavelength. Measurements of the electric field reveal approximately a 60 dB enhancement of the ES fields over the evanescent EM field at regions near the critical density, $\omega_p(z_c) = \omega$.

The experiment is performed in a space chamber³ of approximately 2 m diameter and 4 m length in which a quiescent, steady-state, magnetic-field-free plasma is produced by a dc discharge in argon at 10^{-3} Torr. The plasma is contained by multimirror confinement with 10 000

permanent magnets at the interior chamber walls.⁴ An axial density gradient ($1 < n_0 / |\nabla n_0| < 10$ m) is produced by generating the plasma preferentially near one end of the device and by adjusting the mean free path with neutral pressure; radial gradients are avoided by azimuthally symmetric plasma generation and gas feeds. S-band microwaves ($f \approx 2\,000$ MHz, $\lambda_0 \approx 15$ cm) are launched from antennas⁵ at the low-density end of the device and propagate in the direction of the density gradient toward cutoff, $\omega = \omega_p$. In order to reduce multiple reflection the chamber walls are partly covered with microwave absorbers (fine-wire steel wool). The diagnostics consist of axially and radially motor-driven probes with a shielded coaxial magnetic loop for detection of EM waves [$\vec{H}(\vec{r}, t)$], a coaxially fed short-wire dipole antenna for detecting electric fields [$\vec{E}(\vec{r}, t)$], plane Langmuir probes for determining $n_e(\vec{r})$ and kT_e , and a nonlinear scattering dipole for absolute EM field-strength measurements.⁶

The axial density profile and the typical electric field pattern of the EM wave are shown in Figs. 1(a) and 1(b). Effective free-space propagation measurements in the far-field region have been achieved by propagating fast-rise, phase-

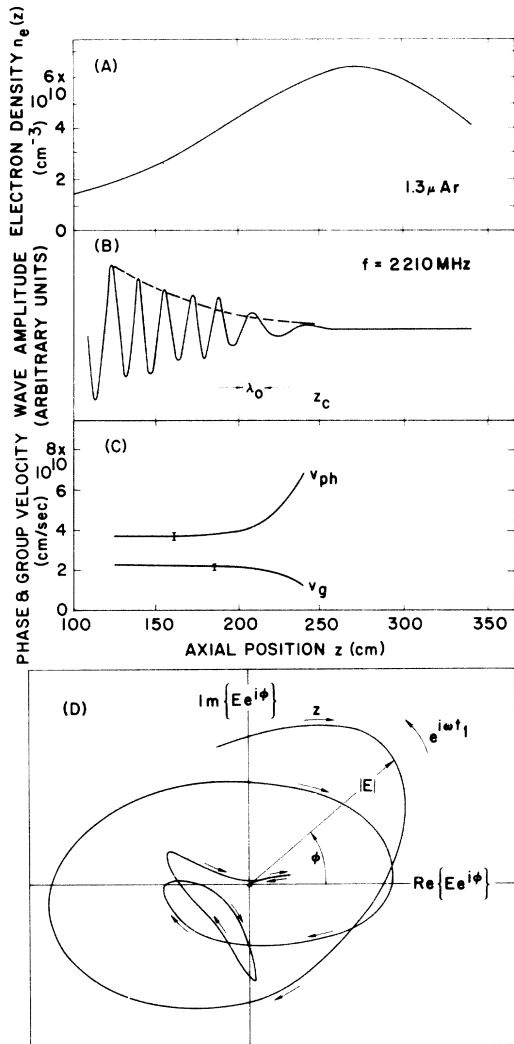


FIG. 1. (a) Axial electron density profile. (b) Spatial dependence of the radial electromagnetic field $E_r(z) \times \cos[\omega t_1 - k(z)z]$, $\omega t_1 = \text{const}$. Dashed line is the theoretical amplitude decay using a three-dimensional ray-tracing program which includes the change in the refractive index. (c) Measured spatial dependence of phase velocity, from (b), and group velocity, from Fig. 2(b). (d) Amplitude and phase of the radial electric field sampled at the same time t_1 at different axial positions. Phase behavior shows the transition from a propagating pattern ($z \ll z_c$) to a standing-wave pattern ($z \approx z_c$).

coherent EM wave bursts and sampling the fields just after the arrival of the fastest wave train corresponding to the straight-line propagation path. Subsequent bursts due to multiple wall reflections have sufficient time delay on account of the large plasma size and do not interfere with the measurement of the main pulse. The ampli-

tude pattern [Fig. 1(b)] clearly shows the increase in wavelength with density and a cutoff at $z = z_c$ where $\omega_p(z_c) = \omega$. The direction of propagation of the EM wave is determined from the phasor plot shown in Fig. 1(d), displaying $|E_r(z) \exp[i(\omega t_1 - kz)]|$ at different axial positions. These data are taken with a sampling oscilloscope (two channels, 90° phase shift) triggered at a fixed time t_1 near the front edge of the EM pulse. The phasor plot shows that the wave propagates towards the cut-off location where wave reflection gives rise to a standing-wave pattern. The unique size of this laboratory plasma also permits the measurement of the group velocity $v_g = \partial\omega/\partial k$, as indicated in Figs. 2(a) and 2(b). As the wave approaches cut-off v_g decreases while the phase velocity increases, in agreement with the theoretical prediction

$$v_g(z) = c^2/v_{ph}(z) = c[1 - \omega_p^2(z)/\omega^2]^{1/2};$$

see Fig. 1(c).

The conservation of energy flux ($v_g E^2 A = \text{const}$, where E is the electric field and A is the illuminated area) implies that the reduction in group velocity gives rise to amplitude swelling as in the usual plane-wave treatment. However, for our divergent beam, refraction causes a strong increase in illuminated area A with increasing distance as a result of the decreasing refractive index $\eta(z) = [1 - \omega_p^2(z)/\omega^2]^{1/2}$.⁷ The net result is an overall reduction in the EM field amplitude near the plasma cutoff as supported by a ray-tracing calculation which includes these two effects [dashed line in Fig. 1(b)]. Further direct evidence for wave refraction is obtained from measurements of the EM field polarization⁶: Near the source the electric field points in the radial direction; near cutoff it rotates by $\Delta\theta \approx 40^\circ$ toward the axis.

The oblique incidence of the EM wave gives rise to an axial electric field $E_{em} \sin\theta$, where θ is the angle between the density gradient n_0' ($= \partial n_0/\partial z$) and the propagation vector of the EM wave. This field is enhanced near z_c according to the following equation derived from the fluid equations and Poisson's equation:

$$\epsilon(z)E_z = k_{D0}^2 E_{em} \sin\theta, \tag{1}$$

where

$$\epsilon(z) = \frac{\partial^2}{\partial z^2} - \frac{n_0'}{n_0} \frac{\partial}{\partial z} + k_{D0}^2 \left(1 - \frac{\omega_p^2(z)}{\omega^2} + \frac{i\nu}{\omega} \right)$$

is a differential operator representing the plasma resonance in a nonuniform plasma in analogy to

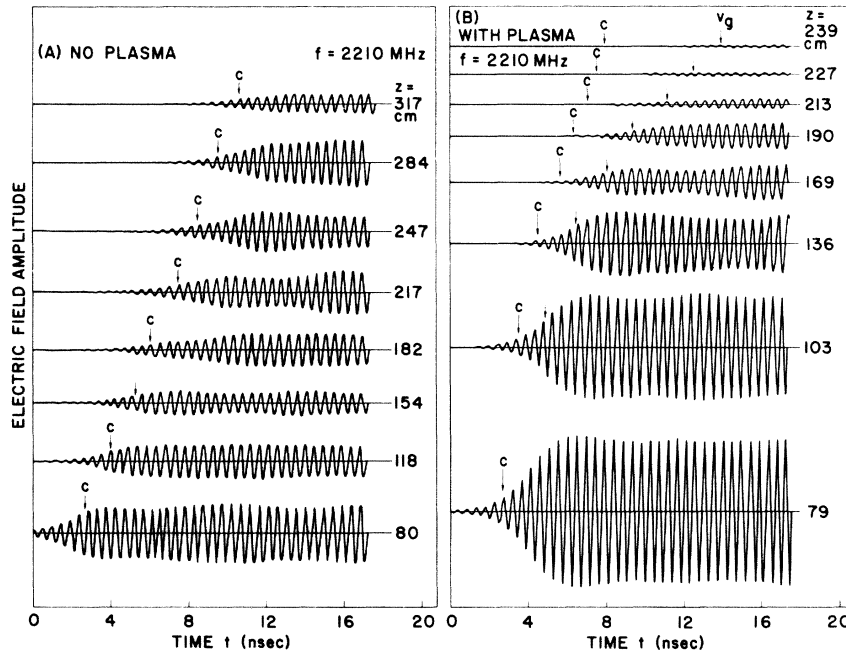


FIG. 2. Time-of-flight measurements with fast-rise phase-coherent microwave bursts. Wave-packet envelope propagates (a) with speed of light (arrow marked "c") in vacuum, (b) with group velocity $v_g < c$ (arrow marked " v_g ") in the plasma. The applied signal in (b) is larger than in (a). Note in (b) the strong decreases in amplitude near cutoff due to plasma refraction effects.

the usual plasma dielectric function in a uniform plasma, and $k_{D0}^2 = \omega^2 m_e / 3\kappa T_e$. The first term of $\epsilon(z)$ represents the propagation of the ES field; the second term, originating from the ambipolar field $\vec{E}_A = (\kappa \Gamma_e / en_0) \nabla n_0$, causes spatial damping in the direction of $-\nabla n_0$; the third term stands for the cold-plasma dielectric effect, with ν being the electron-ion collision frequency. The density gradient allows charge accumulations to occur under this enhanced driving field E_z , and density oscillations δn are excited according to the following equation [derived from Eq. (1) by differentiating it with respect to z , neglecting second-order terms and the spatial dependence of E_{em}]:

$$\epsilon(z) \delta n = -(e/3\kappa T_e) E_z \partial n_0 / \partial z, \quad (2)$$

where the source term on the right-hand side describes the high-frequency density perturbation created by the oscillating field E_z in the presence of the density gradient. Of course, E_z and δn are coupled via Poisson's equation and mutually enhance each other.

In the limit of a gentle density gradient, inspection of Eqs. (1) and (2) shows that the total field E is optimally enhanced from the incident EM field by the factor ω/ν near the resonant location

z_c , where the wavelength of the EM excitation field E_{em} is most closely matched to the excited ES field. At this resonant location electron plasma waves are excited and propagate down the density gradient ($-\nabla n_0$ direction) since the "up-hill" propagation ($+\nabla n_0$) is prohibited by the plasma cutoff. Inspection of $\epsilon(z)$ shows that the excited ES waves should have shorter and shorter wavelengths as they propagate down the density gradient, as given by the approximate relation $k^2 = k_{D0}^2 [1 - \omega_p^2(z)/\omega^2]$.

Probe measurements are performed off the axis ($r > 0$) where the EM wave is oblique to the density gradient. We observe that the cutoff occurs at $z_\theta < z_c$, approximately where $\omega_p(z_\theta) = \omega \cos \theta$. Associated with the axial electric field we find with a thin-wire probe (0.1 mm) electron plasma waves of short wavelengths in the region between EM wave cutoff (z_θ) and z_c . A typical interferometer trace is shown in Fig. 3(a). A phasor plot similar to Fig. 1(d) reveals that the oscillation is a standing wave near resonance z_c , but for $z < z_c$ it goes over into a wave propagating in the $-\nabla n_0$ direction. The spatial dependence of the wave number $k(z)$ shown in Fig. 3(c) agrees with the WKB approximation $k^2(z) = [\omega^2 - \omega_p^2(z)] / (3\kappa T_e / m_e)$ in the region well below the resonance

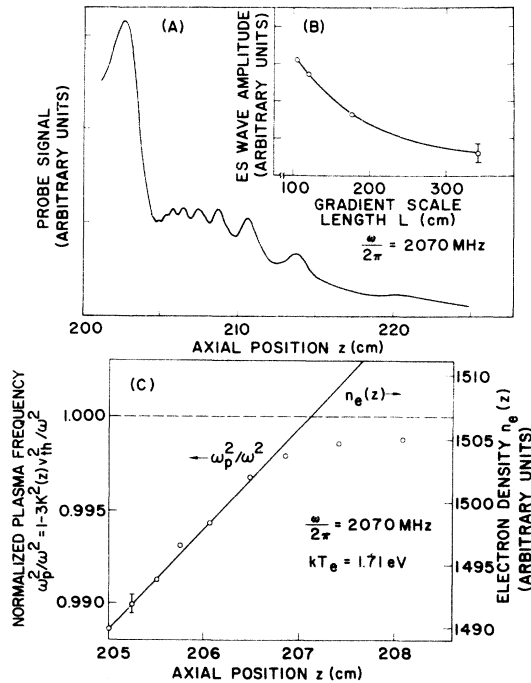


FIG. 3. (a) Receiver-probe signal versus position beyond EM wave cutoff at oblique incidence showing excitation of short-wavelength ES electron plasma waves. (b) Relative ES wave amplitude versus density-gradient scale length L . Normalized plasma frequency (Bohm-Gross) deduced from measured wave number $k(z)$ agrees with that obtained from direct measurement of axial densities except for locations very close to the resonance.

where the approximation holds. The measured density profile which is linear over the short propagation distance has the same gradient scale length as inferred from the measurements of the wave number. The measured dependence of the linearly converted waves as a function of the density-gradient scale length is shown in Fig. 3(b). In the present parameter region we find that the conversion from EM to ES waves is more efficient at steeper density gradients.³

In order to avoid perturbations by the probe on the ES wave a remote method is devised for estimating the resonant ES wave amplitudes. The method is based on the ponderomotive force,⁹ $\nabla \langle E^2 \rangle / 8\pi$, which expels electrons from the resonant region. Ions follow so as to preserve space-charge neutrality, resulting in a density perturbation Δn in the resonant region given by $\Delta n/n_0 = E^2 / 8\pi n_0 kT_e$. After turnoff of a pulsed incident EM wave the associated density perturbation ($\Delta n/n \approx 4\%$ at 10 W incident power) propagates

out from the high-field-strength region and is measured with a Langmuir probe a few centimeters away from the resonance region in the absence of high-frequency signals. We have verified that $\Delta n/n_0$ varies linearly with E^2 and that no ionization takes place. This observation yields local resonant electric field strengths $E_{es} \approx 100$ V/cm which are 3 orders of magnitude above the local EM fields.¹⁰ The conversion efficiency $E_{es}/E_{em} = 10^3$ agrees with the enhancement factor computed exactly¹¹ from Eq. (1) using $\nu/\omega \approx 10^{-4}$ and $L = 100$ cm.

We wish to acknowledge useful discussions with Dr. D. Arnush, Dr. J. Dawson, Dr. B. D. Fried, Dr. C. F. Kennel, and Dr. G. Morales. The able assistance by Mr. M. Plummer is greatly appreciated.

*Work supported by Rome Air Development Center under Contract No. F30602-72-C-0304.

†Fannie and John Hertz Foundation Fellow.

¹M. M. Mueller, Phys. Rev. Lett. **30**, 582 (1973); R. B. White, C. S. Liu, and M. N. Rosenbluth, Phys. Rev. Lett. **31**, 520 (1973); D. L. Kelley and A. Banos, Jr., Plasma Physics Group, University of California, Los Angeles, Report No. PPG 125, 1972 (unpublished).

²N. G. Denisov, Zh. Eksp. Teor. Fiz. **31**, 609 (1956) [Sov. Phys. JETP **4**, 544 (1957)]; A. D. Piliya, Zh. Tekh. Fiz. **36**, 818 (1966) [Sov. Phys. Tech. Phys. **11**, 609 (1966)].

³A. Y. Wong, R. L. Stenzel, D. Arnush, B. D. Fried, C. F. Kennel, and H. Reim, Bull. Amer. Phys. Soc. **17**, 1017 (1972).

⁴R. Limpaecher and K. R. MacKenzie, Rev. Sci. Instrum. **44**, 726 (1973).

⁵A low-gain ($G = 2.7$ dB), wide-angle (H -plane 3-dB beam width $\theta \approx 56^\circ$), rectangular, open-wave-guide antenna has been used for far-field EM wave-propagation studies. Qualitatively similar results are obtained with a large-aperture parabolic antenna ($G \approx 26$ dB, $\theta \approx 14^\circ$). For antenna patterns see S. Silver, *Microwave Antenna Theory and Design* (McGraw-Hill, New York, 1949).

⁶R. L. Stenzel, Rev. Sci. Instrum. (to be published).

⁷In the case of a focused laser beam the refractive effects of a nonuniform plasma will enhance the beam convergence near the focal spot.

⁸This dependence cannot be predicted by Eqs. (1) and (2) in their present simple form, unless the spatial evanescence of the exciting EM field is taken into account.

⁹A. Y. Wong and G. Schmidt, Plasma Physics Group, University of California, Los Angeles, Report No. PPG 151, 1973 (unpublished).

¹⁰Strong enhancements have also been reported by M. P. Bachynski and B. W. Gibbs, Can. J. Phys. **49**, 322 (1971). However, no measurements of electrostatic waves have been reported.

¹¹G. Morales, private communications.